Available online at www.sciencedirect.com

ScienceDirect

Physics Procedia 8 (2010) 2–9

Physics Procedia

www.elsevier.com/locate/procedia

VI Encuentro Franco-Español de Química y Física del Estado Sólido
VI[ème] Rencontre Franco-Espagnole sur la Chimie et la Physique de l'État Solide

Nanostructured $Gd_{0.8}Sr_{0.2}Fe_{0.8}M_{0.2}O_3$ (M = Cr, Ga) Materials for Solid Oxide Fuel Cell Cathodes

I. Ruiz de Larramendi[a], R. Pinedo[a], N. Ortiz-Vitoriano[a], J.I. Ruiz de Larramendi[a], M.I. Arriortua[b], T. Rojo[a, 1*]

[a]*Departamento de Química Inorgánica, Universidad del País Vasco UPV/EHU, Apdo. 644, 48080 Bilbao (España)*
[b]*Departamento de Mineralogía y Petrología, Universidad del País Vasco UPV/EHU, Apdo. 644, 48080 Bilbao (España)*

Abstract

Polycrystalline samples of $Gd_{0.8}Sr_{0.2}Fe_{0.8}M_{0.2}O_3$ (M = Cr, Ga) are prepared by combustion route and pore wetting technique in order to compare the influence of the morphology in the performance of two cathodes for Solid Oxide Fuel Cells. When polycarbonate membranes are used as templates nanowire arrays with a diameter of 50-70 nm are obtained. Comparing the results obtained by Electrochemical Impedance Spectroscopy (EIS) measurements, it is clearly observed that the cathodic resistance considerably decreases when optimized synthesis parameters are used, obtaining a better performance for the $Gd_{0.8}Sr_{0.2}Fe_{0.8}Ga_{0.2}O_3$ nanowires with an area specific resistance (ASR) value at 850ºC of 0.195 $\Omega \cdot cm^2$.

Keywords: impedance spectroscopy; perovskite; nanowire.

1. Introduction

Fuel cells - which, essentially, are electrochemical devices that convert chemical energy in electricity - constitute one the most promising alternatives for the production of environmentally friendly energy. Among them, the so-called SOFCs (solid oxide fuel cells) are characterized by the use of a solid oxide material as electrolyte and by their ability to use any fuel as long as hydrogen is present in its composition [1]. For an optimal functioning, their components must fulfill a series of requisites: (i) the electrolyte must show high ionic but negligible electronic conductivities; the electrode material, on the other hand, must show good conductivity, both ionic and electronic. It should also be porous, in order to allow the access of O_2 to the electrolyte, and be able to catalyze the reactions that take place inside it. (ii) All components of the cell must be thermally and mechanically compatible from room temperature to the working temperature [2]. The progress in this regard has been enormous in the recent years.

* Corresponding author. Tel.: +34-94-601-2458; fax: +34-94-601-3500.
E-mail address: teo.rojo@ehu.es.

1875-3892
doi:10.1016/j.phpro.2010.10.002

However, a number of issues remain that need addressing in the design of SOFCs such as improving the device efficiency and lowering its cost [3], and reducing its working temperature, which, currently, is of the order of 900-1000 ºC for most SOFCs [4,5]. In this sense, a series of compounds with $Ln_{0.7}Sr_{0.7}Fe_{0.8}Co_{0.2}O_3$ (Ln = La, Pr, Gd) formula for the use as cathodes in SOFCs has shown promising results at 600 ºC when tested in prototype cells [6]. Particle size has also been found to play an important role in the performance of the different components of a SOFC. Thus, for example, reducing the particle size of the material used as electrolyte has been found to improve its electrochemical properties significantly [7]. Being able to correlate the new morphologies generated at the nanoscale with the properties of electrolyte and electrode materials is therefore of fundamental interest. Nanostructured components are not stable at the high working temperatures of current SOFCs as the particle size increases significantly with increasing temperature. However, they can be stabilized by reducing the working temperature to 500-800 ºC [8-12]. In this work we present the influence of the morphology of the material on the transport properties of the $Gd_{0.8}Sr_{0.2}Fe_{0.8}M_{0.2}O_3$ (M = Cr, Ga) cathodes together with the development of new nanostructured components for SOFCs.

2. Experimental

2.1. Sample preparation

Powders of $Gd_{0.8}Sr_{0.2}Fe_{0.8}M_{0.2}O_3$ (M = Cr, Ga) were prepared according to combustion synthesis route using glycine as fuel. Appropriate amounts of the nitrate salts [$Gd(NO_3)_3$ $6H_2O$; $Sr(NO_3)_2$; $Fe(NO_3)_3$ $9H_2O$; $Cr(NO_3)_2{\cdot}6H_2O$; $Ga(NO_3)_3$ H_2O] were dissolved in distilled water and glycine was later added to the solution. A concentrated gel was formed when the solution was dried and nitrate-glycine-mixture-gel turns to a vigorous fire, which lasted a few seconds until the combustion process was completed. The resulting powders were calcined first at 800 ºC for 8 hours in air, then pressed into pellets and calcined again at 1300 ºC for 10h.

In order to obtain nanostructured materials, there are generally two approaches to create the desired shapes. One is ‘top down’ which is the fabrication of nanostructures by cutting, etching and milling bulk pieces of materials. The other is ‘bottom up’, which is to grow nanostructures by using catalysis and/or templates. In this work ‘bottom up’ method is used. The $Gd_{0.8}Sr_{0.2}Fe_{0.8}Cr_{0.2}O_3$ (GSFC) and $Gd_{0.8}Sr_{0.2}Fe_{0.8}Ga_{0.2}O_3$ (GSFG) perovskite-type oxide precursor solutions have been synthesized by conventional sol-gel method. Although some other techniques could also be used for this synthesis, the sol-gel technique has been chosen because it enables to prepare very fine powders with a low agglomerating degree. Commercial polycarbonate membranes with a pore diameter of 0.1 and 0.8 μm (Millipore) were used as templates for the formation of the perovskite nanowires by the pore wetting technique. Metal nitrate salts were used as the starting materials for the final product. Citric acid was employed as chelating agent and ethylene glycol as the polymerization agent. $Gd(NO_3)_3{\cdot}6H_2O$, $Sr(NO_3)_2$, $Fe(NO_3)_3{\cdot}9H_2O$, $Cr(NO_3)_2{\cdot}6H_2O$ and $Ga(NO_3)_3{\cdot}H_2O$ (Sigma Aldrich) were weighted stoichiometrically according to the nominal composition of $Gd_{0.8}Sr_{0.2}Fe_{0.8}Cr_{0.2}O_3$ and $Gd_{0.8}Sr_{0.2}Fe_{0.8}Ga_{0.2}O_3$, and then dissolved in distilled water. The volume of added water must be rigorously controlled in order to obtain a homogenously morphology along the sample. Citric acid was then poured into the solution and the resulting mixture was well stirred until it was completely dissolved and after the mixture was completely dissolved. Ethylene glycol was added to the metal citrate solution to promote the esterification in the temperature range between 80 and 100 °C. In this case, the sol-gel solution has not been heated because the gelification prevents the pass of the sample through the pores of the membrane. The sol-gel solution is poured into the membrane until the sample passed through it. The polycarbonate membrane ensures that the sample keeps the desired morphology. The template was removed with a thermal treatment at 600 ºC in air at heating rate of 1 ºC/min which allows the decomposition of the polymer membrane template and reach the crystallization of the compounds. Thus, a new material with nanostructured morphology is obtained for the 0.1 μm template. In contrast, when the 0.8 μm membrane is used, the obtained material is not homogeneously nanostructured, showing some nanowires mixed together with sintered powder. For this reason, in this work only nanostructured samples obtained using 0.1 μm polycarbonate membranes will be studied.

2.2. Characterization of the samples

The crystalline powders were characterized by X ray powder diffraction data, collected using a Philips PW1710 and Philips X'Pert-MPD (Bragg-Brentano geometry) diffractometers, with CuK_α radiation. For microstructure analysis, the obtained powders were examined by field emission scanning electron microscopy (FESEM) with Schottky emitter using a JEOL JSM-7000F microscope at 20 kV accelerating voltage.

Electrochemical Impedance Spectroscopy (EIS) measurements of cathode/yttria-doped zirconia(YSZ)/cathode test cells were conducted using a Solartron 1260 Impedance Analyzer. The frequency range was 10^{-2} to 10^{6} Hz with a signal amplitude of 50 mV. All these electrochemical experiments were performed at equilibrium from 850 ºC down to room temperature, under both zero dc current intensity and air.

3. Results and discussion

XRD patterns for $Gd_{0.8}Sr_{0.2}Fe_{0.8}M_{0.2}O_3$ (M = Cr, Ga) samples prepared by combustion synthesis route were Rietveld-refined on the basis of the existence of two phases (orthorhombic and trigonal phases). Sr doping into the Gd site causes a contraction of the lattice, provoking a structural instability that, in $Gd_{0.8}Sr_{0.2}Fe_{0.8}M_{0.2}O_3$ (M = Cr, Ga) leads to segregation into an orthorhombic (Pbnm) and a trigonal (R-3c) phases as shown in figure 1 [13].

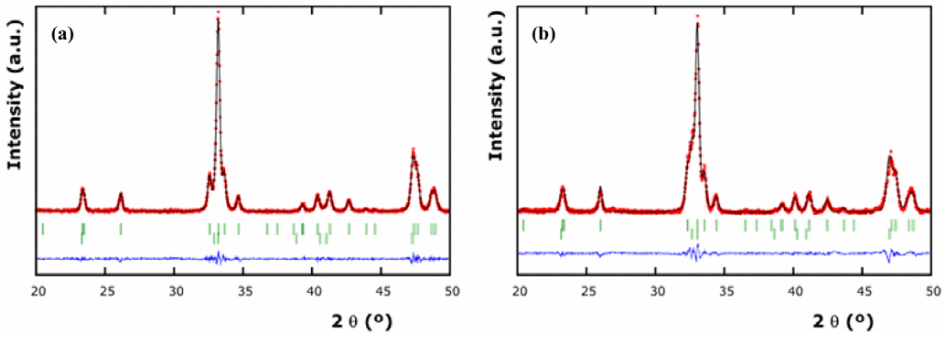

Figure 1. X-ray diffraction patterns of (a) $Gd_{0.8}Sr_{0.2}Fe_{0.8}Cr_{0.2}O_3$ and (b) $Gd_{0.8}Sr_{0.2}Fe_{0.8}Ga_{0.2}O_3$ powders.

At first glance, the diffraction patterns show typical features of a $GdFeO_3$ structure as reported by Kim et al. [14], but a decrease in the intensity of superstructure peaks is observed as the Sr is introduced. This behavior was observed by Blasco et al. [15] in the $Gd_{1-x}Sr_xFeO_3$ series, developing the presence of a miscibility gap with phase segregation for values of $1/8 \leq x \leq 3/5$. The lattice parameters are summarized in table 1.

Table 1. Crystallographic parameters for $Gd_{0.8}Sr_{0.2}Fe_{0.8}M_{0.2}O_3$ (M = Cr, Ga).

M	**Cr**		**Ga**	
S.G.	**Pbnm**	**R-3c**	**Pbnm**	**R-3c**
a (Å)	5.3734(7)	5.4929(2)	5.3653(1)	5.5112(1)
b (Å)	5.5476(7)		5.5648(2)	
c (Å)	7.6764(8)	13.2875(7)	7.6807(4)	13.2650(2)
χ^2	1.22		2.40	

In order to measure the particle size of the samples, scanning electron microscopy (SEM) was used. It is well known that particle size influences on transport properties of the sample, and must be reduced in order to obtain a better behavior of the material as cathode. The microstructure of the obtained particles via the combustion route

reveals no uniform grain growth. The recorded images can be visualized in Fig. 2. The combustion synthesis gives rise to a grain size of about 0.5-1 μm but all the particles are forming conglomerates showing a variety of inhomogeneous particle sizes. The reason for this behavior is the very high temperature needed to obtain desired materials.

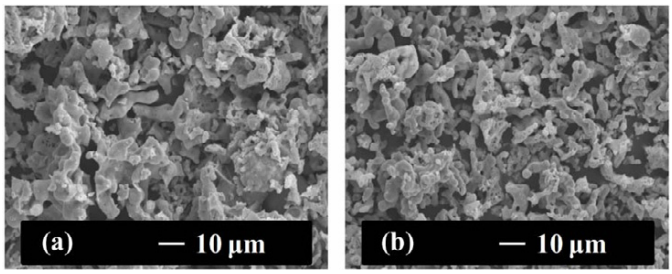

Figure 2. Surface view of the microstructure of the porous (a) $Gd_{0.8}Sr_{0.2}Fe_{0.8}Cr_{0.2}O_3$ and (b) $Gd_{0.8}Sr_{0.2}Fe_{0.8}Ga_{0.2}O_3$ powders.

Scanning electron microscopy (SEM) images of GSFC and GSFG nanostructures grown using 0.1 μm polycarbonate membranes as templates at 600 ºC are shown in figure 3. An homogeneous growth of nanowires is clearly observed. The lengths of the nanowires are about 2 - 4 μm with a diameter of 50 - 70 nm, much smaller than that of the polycarbonate templates. Microstructure and morphology (i.e. crystallite and particle size, porosity, electrode/electrolyte interface, etc.) of cathodes play a key role on its polarization resistance, because when the surface area of the electrode is increased, a large amount of double-phase-boundaries (where gas and cathode meet) and triple phase boundaries (regions where electrolyte, electrode and gas are in contact) is originated, giving rise to a higher efficiency of the device.

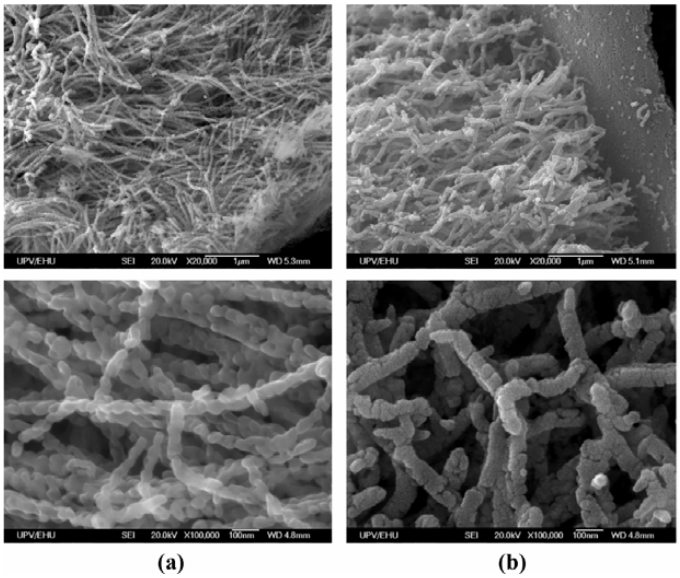

Figure 3. SEM images of (a) $Gd_{0.8}Sr_{0.2}Fe_{0.8}Cr_{0.2}O_3$ and (b) $Gd_{0.8}Sr_{0.2}Fe_{0.8}Ga_{0.2}O_3$ nanostructures formed using polycarbonate templates.

The conducting properties of the sample were studied using a two electrode cell, being necessary to obtain impedance spectra for symmetrical cells. In this way, the cells were made of YSZ electrolyte pellets onto which symmetrical electrodes of GSFC and GSFG materials were painted. Platinum was used as current collector.

The YSZ electrolyte pellets were made using NexTech material as it was received. The powder was pressed under 10 T uniaxial force to form green pellets which were sintered at 1500 ºC for two hours with a density higher than 93% of the theoretical value. The surface of the pellets was polished with sandpaper and then cleaned with ethanol and acetone solutions. The powders of GSFC and GSFG electrodes were dispersed in a vehicle ink forming a paste which was painted with a paintbrush on both faces of the pellets forming symmetrical cells. These cells were sintered at 1050 ºC for one hour with a 10 ºC/min rate to form porous electrodes well adhered to the surfaces of the electrolyte.

A complex impedance spectroscopy study of the transport properties of $Gd_{0.8}Sr_{0.2}Fe_{0.8}M_{0.2}O_3$ (M = Cr, Ga) allowed an initial evaluation of the different processes involved in the electrical conduction in these materials. Nyquist plot of GSFC/YSZ half cell measured at 300 ºC is shown in figure 4. In this figure, the different processes observed at low temperatures are described and only contributions due to the electrolyte can be seen. Preliminary results obtained from the material used as electrolyte (yttria-stabilized zirconia -YSZ-) show three fundamental contributions (see fig. 4): i) one related to the conduction inside the grains (bulk), ii) one due to the grain boundary (g.b.) processes and iii) the attributed to charge transfer between the electrolyte material and the electrodes. However, the contribution of the processes taking place in the electrode (interface processes, electrode reactions, etc.) is better observed at high temperatures.

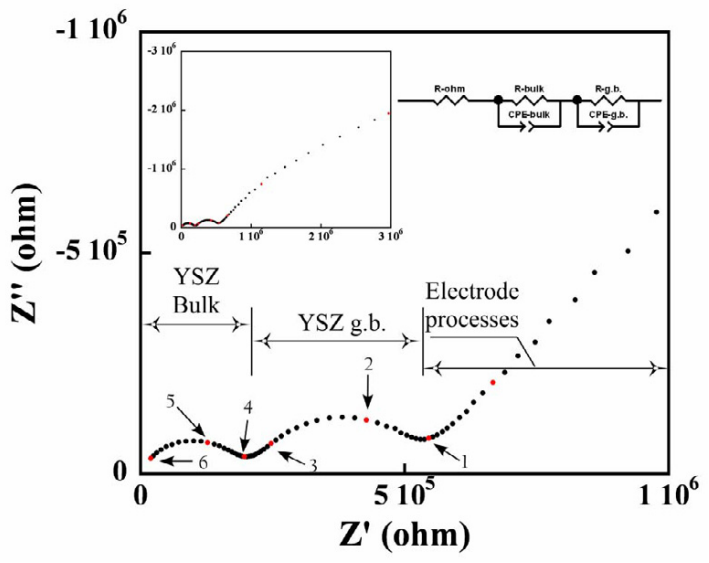

Figure 4. Typical impedance diagrams obtained with GSFC/YSZ half cell, under air, at 300 ºC. The numbers in this plot correspond to logarithm of frequency.

At high frequencies the semicircle appears due to the bulk of the compound, with a value of capacitance of $4{,}78 \cdot 10^{-12}$ F. The following semicircle that is observed at not so high frequencies is due to the grain boundary of the electrolyte, with a capacitance of $2{,}41 \cdot 10^{-9}$ F. These values agree with the obtained ones of the bibliography [16].

Electrochemical impedance spectra for GSFG/YSZ/GSFG cells prepared with powders and nanowires are reported in the Nyquist plan at 800 ºC (Fig. 5), being distinguishable three main arcs. These data were successfully fitted to an equivalent circuit shown in figure 5c.

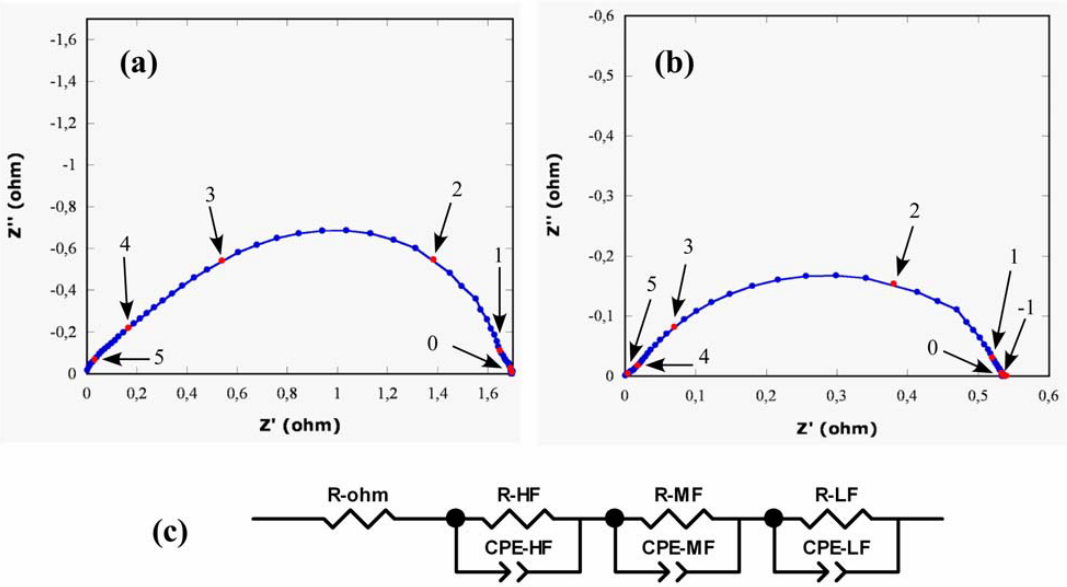

Figure 5. Impedance spectra of $Gd_{0.8}Sr_{0.2}Fe_{0.8}Ga_{0.2}O_3$ (a) powders and (b) nanowires measured under air at 800 ºC. (c) Equivalent circuit for fitting the impedance spectra (HF: High Frequencies; MF: Medium Frequencies; LF: Low Frequencies). The impedance data are plotted after electrolyte ohmic drop correction. The numbers in (a) and (b) plots correspond to logarithm of frequency.

The Nyquist plots were fitted on the basis of an equivalent circuit constituted of resistance-constant phase elements (R-CPE) in parallel associated in series. The calculated equivalent capacitance values were on the order of 10^{-4} F cm^{-2} for the high frequency arcs, 10^{-3} F cm^{-2} for the medium frequency arcs and in the range 0.1 – 0.6 F cm^{-2} for the low frequency arcs. Resistances values assigned to the different processes are listed in table 2.

Table 2. Resistance values for the $Gd_{0.8}Sr_{0.2}Fe_{0.8}Ga_{0.2}O_3$ sample at 800 ºC.

Resistance (ohm cm^2)	Powder	Nanowire
R - HF	0.241	0.082
R - MF	0.436	0.142
R - LF	0.145	0.046

The processes related to high frequencies contribution is attributed to charge transfer followed by the ionic incorporation into the electrolyte. At medium frequencies the surface diffusion of oxygen is observed, while at low frequency process is probably related to gas diffusion [17]. The three contributions showed lower resistances when nanostructured electrodes were used. This behavior becomes more relevant for the processes assigned to the high and low frequencies. The HF contribution related to the creation of TPB (Triple Phase Boundaries) sites, where electron, ion and gas meet, facilitates the incorporation of oxide ions to the electrolyte. On the other hand, when nanostructured electrodes were used, in addition to the creation of TPB sites, also DPB (Double Phase Boundaries)

sites where the electrode meets with the gas phase are generated. This fact improves the gas diffusion lowering the LF resistance.

Using the electrodic resistance (the diameter of the arc associated with the cathode response), $R_{electrode}$, the cathodic Area Specific Resistance (ASR) can be deduced from the relation: ASR = $R_{electrode}$ × Surface / 2. The obtained values of the ASR are given in table 3.

Table 3. Values of ASR (ohm cm^2) for $Gd_{0.8}Sr_{0.2}Fe_{0.8}M_{0.2}O_3$ (M = Cr, Ga) electrodes with the YSZ electrolyte.

Temperature	M = Cr		M = Ga	
(ºC)	Powder	Nanowire	Powder	Nanowire
850	0.842	0.286	0.534	0.195
800	1.461	0.567	0.824	0.272
750	2.869	1.435	1.490	0.745

As shown in table 3, the $Gd_{0.8}Sr_{0.2}Fe_{0.8}Ga_{0.2}O_3$ nanostructured electrode exhibits under open-circuit conditions the lowest area-specific apparent polarization resistance ($R_{electrode}$), determined by the intersection of each impedance spectrum in the Nyquist plots with the Z' axis. In a conventional cathode (powder), it is difficult for oxygen ions to cross the interface and to travel within the cathode. When nanostructured material is used as cathode, the increase of the number of TPB sites (favoring the oxygen ion incorporation) may be one of the reasons for the reduced ASR of the nanostructured samples compared with the conventional electrode obtained from combustion synthesis.

4. Conclusion

In this study, the $Gd_{0.8}Sr_{0.2}Fe_{0.8}M_{0.2}O_3$ (M = Cr, Ga) phases were prepared by two different routes: combustion synthesis and pore wetting technique. X-ray diffraction patterns showed segregation into an orthorhombic (Pbnm) and a trigonal (R-3c) phases. The morphology of the materials synthesized by both routes is quite different. While powders synthesized by the combustion method showed a grain size of about 0.5-1 μm forming agglomerates, an array of nanowires with a diameter of 50 - 70 nm is obtained using the pore wetting technique. So, we found that nanostructured materials can be obtained with the pore wetting technique. Nanowires of many types of materials can be grown in solution, which has the advantage that can be scaled-up to produce very large quantities of nanowires as compared to other methods that produce nanowires on a surface.

The electrochemical properties of the $Gd_{0.8}Sr_{0.2}Fe_{0.8}M_{0.2}O_3$ (M = Cr, Ga) cathodes strongly depend on the microstructure and morphologies. Impedance spectroscopy measurements showed that cathode polarization resistance can decrease considerably if optimized synthesis parameters are used. A better performance for the $Gd_{0.8}Sr_{0.2}Fe_{0.8}Ga_{0.2}O_3$ nanowires with an ASR value at 850 ºC of 0.195 $\Omega \cdot cm^2$ measured in a two electrode configuration using symmetrical cells is obtained. This way, nanostructured electrodes, especially cathodes, of SOFCs can give rise to a better performance of the fuel cells.

5. Aknowledgements

This work has been partially financed by the Spanish CiCyT under project MAT2007-66737-C02-01 and by the Government of the Basque Country under project IT-312-07. I. Ruiz de Larramendi gratefully acknowledges the Government of the Basque Country for funding her research activities as postdoc within the Project GIC07/126-IT-312-07. R. Pinedo thanks the Universidad del País Vasco/Euskal Herriko Unibertsitatea for his predoctoral fellowship and N. Ortiz-Vitoriano thanks the Eusko Jaurlaritza/Gobierno Vasco for her predoctoral fellowship.

References

[1] B.C.H. Steele and A. Heinzel, Nature 414 (2001) 345.
[2] S.C. Singhal, Solid. State Ionics 135 (2000) 305.

[3] S. Obara, Int. J. Hydr. Energy 35 (2010) 757.
[4] A. Tarancón, Energies 2 (2009) 1131.
[5] Z. Gao, J. Huang, Z. Mao, C. Wang and Z.Liu, Int. J. Hydr. Energy 35 (2010) 731.
[6] I. Ruiz de Larramendi, D.G. Lamas, M.D. Cabezas, J.I. Ruiz de Larramendi, N.E. Walsöe de Reca and T. Rojo, J. Power Sources 193 (2009) 774.
[7] M.G. Bellino D.G. Lamas and N.E. Walsöe de Reca, Adv. Funct. Mater. 16 (2006) 107.
[8] M.G. Bellino, J.G. Sacanell, D.G. Lamas, A.G. Leyva and N.E. Walsöe de Reca, J. Am. Chem. Soc. 129 (2007) 3066.
[9] S. Barison, M. Battagliarin, T. Cavallin, S. Daolio, L. Doubova, M. Fabrizio, C. Mortalo, S. Boldrini and R. Gerbasi, Fuel Cells 8 (2008) 360.
[10] M. Darab, M.S. Toprak, G.E. Syvertsen and M. Muhammed, J. Electrochem. Soc. 156 (2009) K139.
[11] J. Sacanell, A.G. Leyva, M.G. Bellino and D.G. Lamas, J. Power Sources 195 (2010) 1786.
[12] S. Wang, J. Yoon, G. Kim, D. Huang, H Wang and A.J. Jacobson, Chem. Mater. 22 (2010) 776.
[13] K. Kammer, Solid State Ionics 177 (2006) 1047.
[14] C.S. Kim, Y.R. Um, S.I. Park, S.H. Ji, Y.J. Oh, J.Y. Park, S.J. Lee and C.H. Yo, IEEE Trans. Magn. 30 (1994) 4918.
[15] J. Blasco, J. Stankiewicz and J. García, J. Solid State Chem. 179 (2006) 898.
[16] J.T.S. Irvine, D.C. Sinclair and A.R. West, Adv. Mater. 2 (1990) 132.
[17] Z. Jiang, Z. Lei, B. Ding, C. Xia, F. Zhao and F. Chen, Int. J. Hydrogen. Energ. 35 (2010) 8322.